Modeling of an ion source lens system for sensitivity enhancement in a non-scanning linear ion trap

Boris Brkić [a,*], Stamatios Giannoukos [a], Neil France [b], Aurika Janulyte [c], Yves Zerega [c], Stephen Taylor [a]

[a] Department of Electrical Engineering and Electronics, University of Liverpool, Brownlow Hill, Liverpool L69 3GJ, United Kingdom
[b] Q Technologies Ltd, 100 Childwall Road, Liverpool L15 6UX, United Kingdom
[c] Equipe IPCN, Aix-Marseille Université, Centre de Saint Jérôme – Bât MADIREL, 13397 Marseille Cedex 20, France

ARTICLE INFO

ABSTRACT

This article presents a novel simulation study for improving the sensitivity of linear ion trap mass spectrometers used for sensing low sample concentrations in field applications. Commercial simulation software using the boundary element method has been used for modeling ion source lens system for externally created ions, which are then injected into a 2D linear ion trap mass analyzer operating in a non-scanning mode. The geometric parameters of the ion source lens system were varied to investigate the effects on ion trap sensitivity by altering the number of ions injected into the analyzer and their focus. The performance results are given for cocaine (*m/z* 182 and 304) ions, showing significant improvement in sensitivity when the optimized lens system is used.

© 2013 Elsevier B.V. All rights reserved.

1. Introduction

The growing trend towards portable mass spectrometry has already brought portable systems for environmental applications, such as detection of toxic compounds in air [1] and oil-in-water monitoring [2]. High demand from the security sector for artificial sensing of illegal substances has created a potential for detection of narcotics [3] and explosives [4] using miniature mass spectrometers. The main driver for hardware realization of portable systems has been a miniaturization of the mass analyzer – the key component of every mass spectrometer. A smaller analyzer can operate at higher pressures due to shorter ion mean free path, requiring less robust vacuum system, which reduces size and weight of a system. Miniaturization also enables analyzer operation at lower voltages, which reduces power consumption necessary for a portable system. The three types of mass analyzers that have been successfully miniaturized include quadrupole mass filter [5–7], ion trap [8–10] and time-of-flight [11–13]. The ion trap is the most commonly used analyzer in portable systems due to capability to perform mass analysis at higher pressures than other analyzers and it offers a relatively high mass range (*m/z* to 2000). This allows battery-powered instruments at lower cost, size and weight with extended number of applications.

This work is involved with simulating performance of an ideal linear ion trap (LIT) with a coupled ion source lens system (ISLS) for ion injection and focusing. The LIT is a 2D trap with linear quadrupole electric field along axial (*z*) direction. The field linearity provides better performance for an LIT than for 3D types of ion traps (e.g., quadrupole ion trap) [14]. The main advantages include better sensitivity and faster mass scanning. This is because linear axial field enables 'smoother' forward and backward ion oscillations, which results in more ions remaining stable during trapping and ejected faster during scanning [15–17]. Sensitivity in portable LIT mass spectrometers is commonly optimized with the design of a mass analyzer and signal-to-noise ratio of the detector (usually electron multiplier). Optimization of geometry and increase in the size of an analyzer, increase the capacity to store ions leading to higher sensitivity. Likewise, higher gain multiplier detectors further improve sensitivity. However, both of these factors have their limitations. LIT size can be increased to the level determined by electrode voltages required to achieve the targeted mass range for a given size. In similar way, multiplier gain can only be increased to a level where signal is clearly distinguished from the noise. Another option for sensitivity enhancement is to improve ion injection and focusing to further increase the number of trapped and ejected ions. This can be done through optimized design of an ISLS, which is investigated in this paper.

The following sections describe characteristics of a nonscanning LIT, modeling method and ISLS with simulation results presented for ion injection, trapping and ejection. The advantage

of using a non-scanning LIT to achieve high sensitivity for targeted substances is explained with experimental results shown for the Liverpool LIT. The accuracy and suitability of the boundary element method for this study are discussed. Functionality of the ISLS is explained with modeling parameters given. Simulation results are shown for cocaine (*m/z* 182 and 304) ions for a range of geometric parameters of the ISLS including ion trajectories for commercial and simulation-optimized lens systems. High impact of the ISLS geometry on sensitivity of the mass analyzer is demonstrated, showing significant potential for sensitivity enhancement through optimized ion injection and focusing.

2. Experimental

2.1. Non-scanning linear ion trap

Mass analysis in ion traps is usually achieved through voltage scanning on the trap electrodes. In this way, confined ions are selectively ejected from the trap from lowest to highest mass-to-charge ratio (*m/z*) to generate mass spectrum across the defined mass range. In LITs, voltage scanning is done by ramping the RF voltage amplitude on the quadrupole rods in sequence with ramping bias voltages on the rods [18,19]. Bias voltage is either a low value DC or low amplitude AC voltage held at a constant ratio with RF voltage and it is used to isolate individual ion masses. Fine mass resolution of spectral peaks is achieved by varying the scan time, where longer scan times give higher resolutions.

In portable applications for which only specific substances have to be monitored (e.g., few spectral peaks), common mass analysis through scanning may not be the best choice. The main reasons are lower sensitivity and complicated drive electronics due to the voltage scanning circuitry involved. All scanning methods begin at one fixed RF voltage (low cut-off point) to trap all the ions across the defined mass range. This trapping RF voltage may be optimal for a few ion masses, but it will not be optimal for most other masses, which can cause a significant loss of ions during trapping and reduce sensitivity. Apart from ion losses during trapping, many ejected ions are lost during scanning when the trapping RF voltage is ramped. This is because of the nature of the mass scanning, where the trade-off between trapping and scanning voltages is created to maintain higher ion masses confined during ejection of a lower ion mass.

An alternative mass analysis scheme for portable sensing is to use a non-scanning method, where no voltage ramping is performed [20]. In a non-scanning method, for each run, only one specific targeted ion mass is confined and ejected at a time. In this way, every mass that is monitored can have optimal trapping and ejection voltages applied, which increases instrument sensitivity. Removal of scanning circuits also simplifies circuitry design, reduces power consumption and overall cost of the drive electronics.

Fig. 1 shows a schematic diagram of a non-scanning ideal LIT with hyperbolic electrodes designed at University of Liverpool. It operates by axially injecting ions into the trap using the ISLS, where one specific ion mass is trapped and axially ejected at a time. Selective ion trapping is performed by applying suitable positive RF voltage to the *y*-axis quadrupole rods (*y*-electrodes), and negative and positive DC biases to the *x*- and *y*-axes rods (*x*,*y*-electrodes) respectively. Ion extraction of positive ions is achieved by switching the positive DC voltage on the exit endplate (exit *z*-electrode) to a suitable negative value, enabling maximum number of ions at the target mass to be ejected.

To isolate a single ion mass, the LIT must be operating near the tip of its stability diagram. Fig. 2 shows the stability diagram for an ideal 2D LIT, which is identical to the one for a quadrupole mass
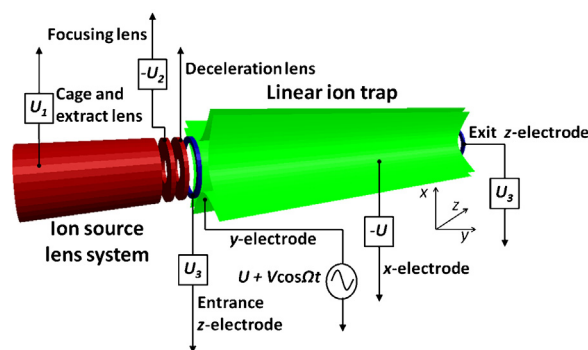

Fig. 1. Schematic diagram of a non-scanning linear ion trap with a coupled ion source lens system.

filter [21]. The stability diagram is mathematically represented with dimensionless parameters a_u and q_u, whose values for single mass trapping are slightly below 0.706 and 0.237 respectively. The DC and RF voltages required for isolation of a single charged positive ion mass for the LIT in Fig. 1 are given by:

$$U = a_u m r_0^2 \Omega^2 / 8e \tag{1}$$

$$V = q_u m r_0^2 \Omega^2 / e \tag{2}$$

where U is the total DC bias applied to *x*- and/or *y*-electrodes, m is the ion mass, r_0 is the inscribed radius of electric field, Ω is the angular frequency (equal to $2\pi f$, where f is the frequency of the RF field), e is the elementary charge of an electron and V is peak-to-peak RF amplitude applied to *y*-electrodes.

2.2. Experimental mass isolation in a non-scanning linear ion trap

Selective mass isolation in a non-scanning mode has been done experimentally using hyperbolic LIT fabricated by the University of Liverpool with the design shown in Fig. 1. The tested LIT was built using CNC machining with electrodes made from stainless steel and electrode holders made from ceramic resin. The length of *x*- and *y*-electrodes was 40 mm with 2.5 mm r_0. *z*-Electrodes were 0.4 mm thick discs separated from *x*,*y*-electrodes by 0.8 mm with 2.5 mm aperture radius. A commercial dual thoria filament electron impact ion source was used (SS Scientific Ltd., UK) that was close coupled to LIT providing external ion injection. The detector was channeltron type electron multiplier (Burle, US). Data acquisition was obtained using in-house made charge amplifier connected to oscilloscope.

For experimental mass isolation of Kr-84 and Xe-131 ions, the following parameters were used:

- Ion source: 100 μA electron emission current with 2.2 A filament current and −20 V applied to the repeller/filament common; 100 ms ionization time.
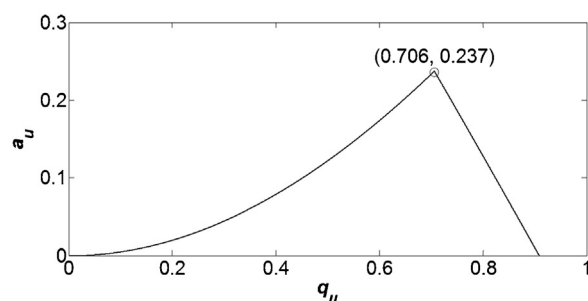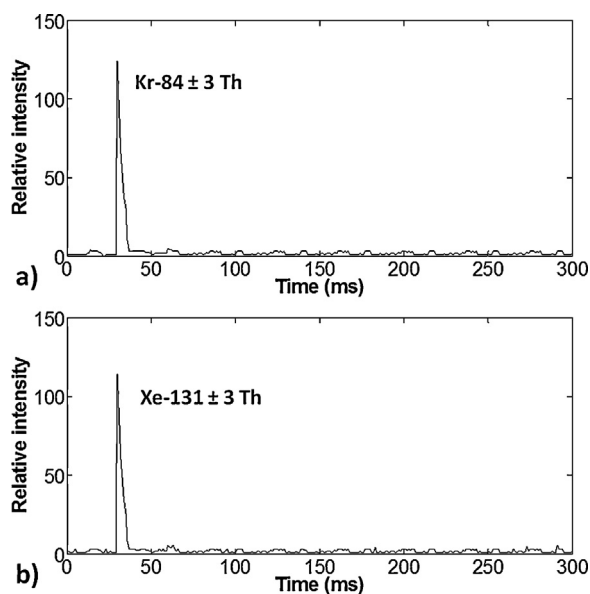

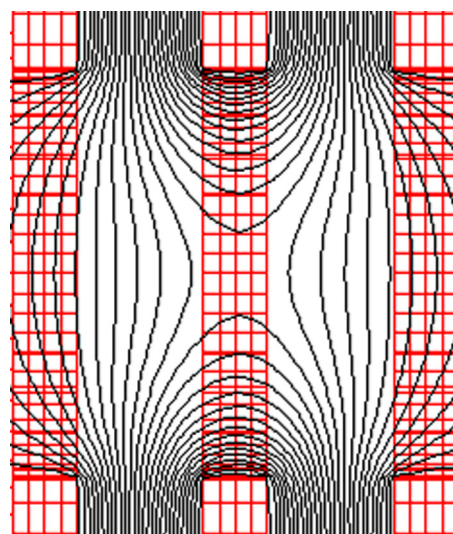**Fig. 2.** Stability diagram for an ideal 2D linear ion trap.

Fig. 3. Experimental selective mass isolation for (a) Kr-84 and (b) Xe-131 within CNC linear ion trap operating in a non-scanning mode. The mass window width obtained is 6 Th.

- LIT: x-electrodes: negative DC bias of −4.2 V for Kr-84 and −6.5 V for Xe-131; y-electrodes: positive DC bias of 4.2 V for Kr-84 and 6.5 V for Xe-131, RF amplitude of 196 V_{p-p} for Kr-84 and 304 V_{p-p} for Xe-131 at 1.14 MHz RF drive frequency; z-electrodes: entrance endplate at 0 V during ion injection, and at 20 V during ion trapping and ejection, exit endplate at 20 V during ion injection and trapping, and at −100 V during ion ejection; 1 ms ion trapping time; 300 ms ion ejection time.
- Detector: multiplier voltage at −1000 V for isolation of both Kr-84 and Xe-131.
- Pressure: typically up to 10^{-4} Torr with a sample gas and helium buffer gas added for optimal signal intensity.

Fig. 3 shows peak intensities for Kr-84 and Xe-131 with mass isolation window width of 6 Th. Upper and lower mass limits of the window were identified by increasing and decreasing RF/DC voltage levels until the mass peak disappeared. The time to completely eject trapped ion masses was 7.5 ms within specified ejection time of 300 ms. With further RF/DC fine adjustments, the mass window width could be reduced to 4 Th, but not much lower. This is because mass peak disappears when RF and DC voltages are very near the tip of the stability diagram. Sensitivity improvement through increase of ionization time could be seen up to 100 ms, while longer ionization times did not give any enhancement in sensitivity. Further enhancement of sensitivity is possible through maximizing number of ions injected into LIT and better ion focusing, which is explained in detail in Section 4.

3. Methods

Performing numerical modeling can be very useful when designing mass spectrometers because the effects on ion motion from electrode geometry alterations can be investigated much quicker and cheaper than in experiments. The simulation results presented here for the ISLS coupled to the non-scanning LIT were done using a 3D version of a commercial software simulation program: charged particle optics (CPO) [22]. CPO is based on the boundary element method (BEM), which was previously shown to be highly accurate for modeling ion motion in miniature ion

traps [23]. CPO also supports space charge simulation, which allows closer approximation to experimental conditions.

The BEM works by numerically solving the charge distribution on the electrode surfaces. The values of these surface charges are used to compute the electrostatic fields and potentials at any point in 3D space between the electrodes. The electrodes drawn using BEM are divided into small segments, which are usually represented by a triangular mesh. Each triangular segment in CPO is assumed to have uniformly distributed amount of constant charge. Segmentation is done only on conducting surfaces rather than complete electrode volumes as in other methods (e.g., finite element and finite difference methods). Because of this feature, BEM is also called surface charge method [24]. Finally, CPO offers high accuracy near the electrode edges, which made it a logical choice for modeling mass spectrometer components.

Fig. 4. Equipotential lines within the ion source lens system.

4. Results and discussion

4.1. Simulation set-up

In our model, a lens system for an external ionization ion source was coupled to an ideal linear ion trap operating in a non-scanning mode (see Fig. 1). The lens system consists of ion extract lens, focusing lens and deceleration lens, which can be used for any type of ion source where ions are created outside of mass analyzer. The system in Fig. 1 is adapted for an electron impact ion source where positive ions are created inside cylindrical cage after sample neutrals were bombarded with electrons from the hot filament. Upon creation, ions are extracted from the cage using extract lens that is connected to the cage with same positive DC voltage applied. Extracted ions are then focused and accelerated using focusing lens held at negative DC voltage. To increase the ability of focused ions to be confined within the trap, their energies are reduced using a grounded deceleration lens.

Fig. 4 shows the equipotential lines within the ISLS with strong controlling effect from the ion focusing lens. Fig. 5 shows the ISLS geometrical parameters that were varied in our simulation study for optimizing the sensitivity of an LIT. These include:

- aperture radius (r_a) of the lenses,
- distance between the deceleration lens and entrance z-electrode (d_d) using the optimal r_a value,
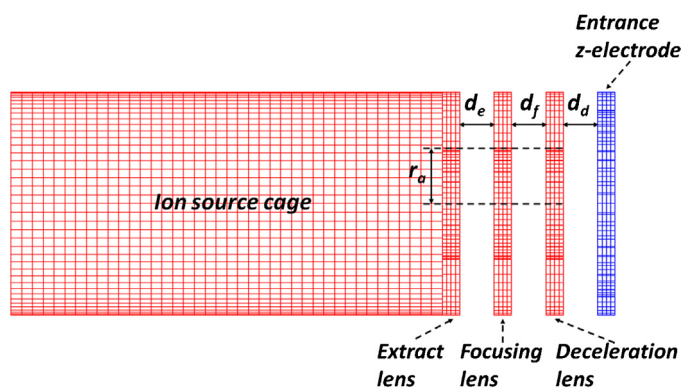
Fig. 5. Geometrical parameters of the ion source lens system varied in simulations.

- distance between focusing and deceleration lenses (d_f) using optimal r_a and d_d,
- distance between extract and focusing lenses (d_e) using optimal r_a, d_d and d_f.

The dimensions for the ISLS geometrical parameters are the following:

- ion source cage: 3 mm radius and 10 mm length,
- lens aperture radius (r_a): varied from 0.25 mm ($0.1r_0$) to 2.5 mm (r_0),
- lens thicknesses (d): 0.4 mm,
- inter-lens distances (d_d, d_f and d_e): varied between 0.8 mm ($2d$) and 4 mm ($10d$).

Note that 0.4 mm lens thickness is a typical thickness of commercially available electrostatic lenses for ion sources. Likewise, the inter-lens distance step of 0.8 mm corresponds to the width of standard commercial ceramic spacers. The defined values for LIT geometrical parameters are therefore:

- x,y-electrodes: 40 mm electrode length with 2.5 mm r_0,
- z-electrodes: 0.4 mm thickness, 2.5 mm aperture radius with 0.8 mm separation from x,y-electrodes.

Simulations were done for most distinguished cocaine fragment masses at m/z 182 and 304 since cocaine detection is a potential application for a portable LIT mass spectrometer. 8000 randomly distributed ions at m/z 182 and 304 were defined within the whole cage area with their initial energy set to 0.01 eV. For each variation of geometrical parameters, three phases of ion motion were simulated: injection, trapping and ejection. Successful ions in each phase were the ones that satisfied the following conditions:

- injection: successful ions must pass through the lens system and enter the LIT,
- trapping: successful ions must remain trapped within the LIT for 1 ms,
- ejection: successful ions must exit the LIT through the aperture on the exit z-electrode.

Note that trapping times in a real portable LIT system would even be shorter in order to maximize sensitivity and detection speed for a targeted substance. The ISLS voltages defined in the model were:

- cage and extract lens: 3 V,
- focusing lens: −70 V,
- deceleration lens: 0 V.

Voltages on the LIT electrodes were chosen as follows:

- x-electrodes: 0 V during injection and trapping with bias voltages during ejection of −6.9 V DC for m/z 182 and −11.5 V DC for m/z 304,
- y-electrodes: 329 V_{p-p} and 549 V_{p-p} at 1 MHz with bias voltages of 6.9 V DC and 11.5 V DC for m/z 182 and 304, respectively,
- entrance z-electrode: 0 V during injection and 20 V during trapping and ejection,
- exit z-electrode: 20 V during injection and trapping, and −20 V during ejection.

RF and DC voltages were calculated from Eqs. (1) and (2). The DC biases on x,y-electrodes were adjusted to create DC potential differences (U voltages), required for trapping specific ion masses.
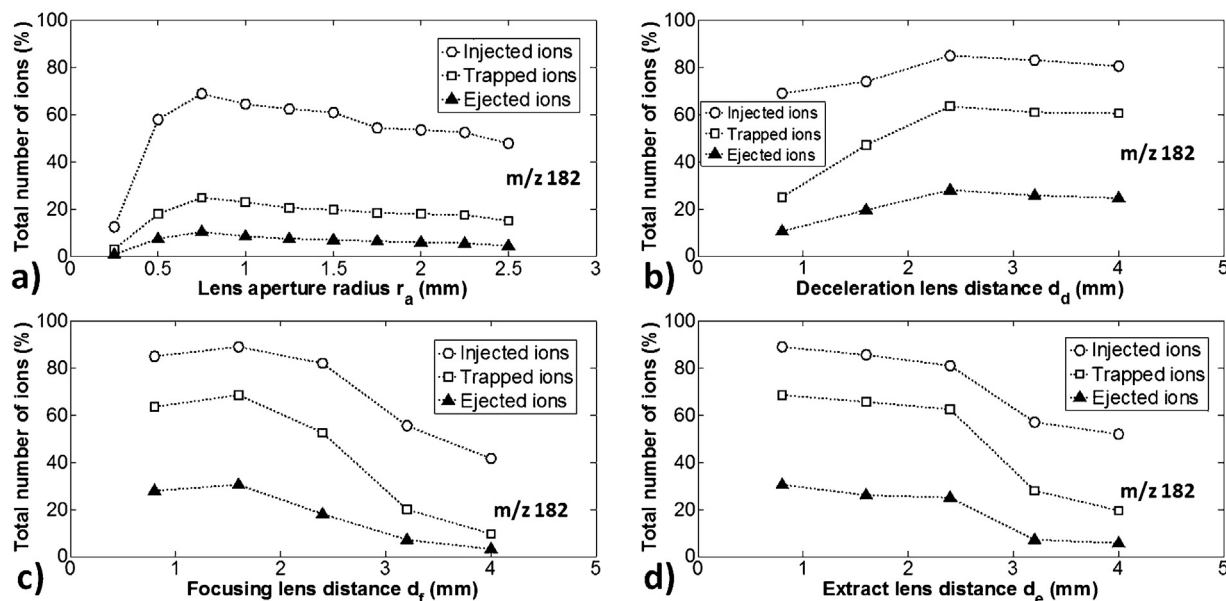

Fig. 6. Effects of varying ISLS geometrical parameters (r_a, d_d, d_f and d_e) on ion injection, trapping and ejection for cocaine at m/z 182 (3D simulations obtained using CPO).
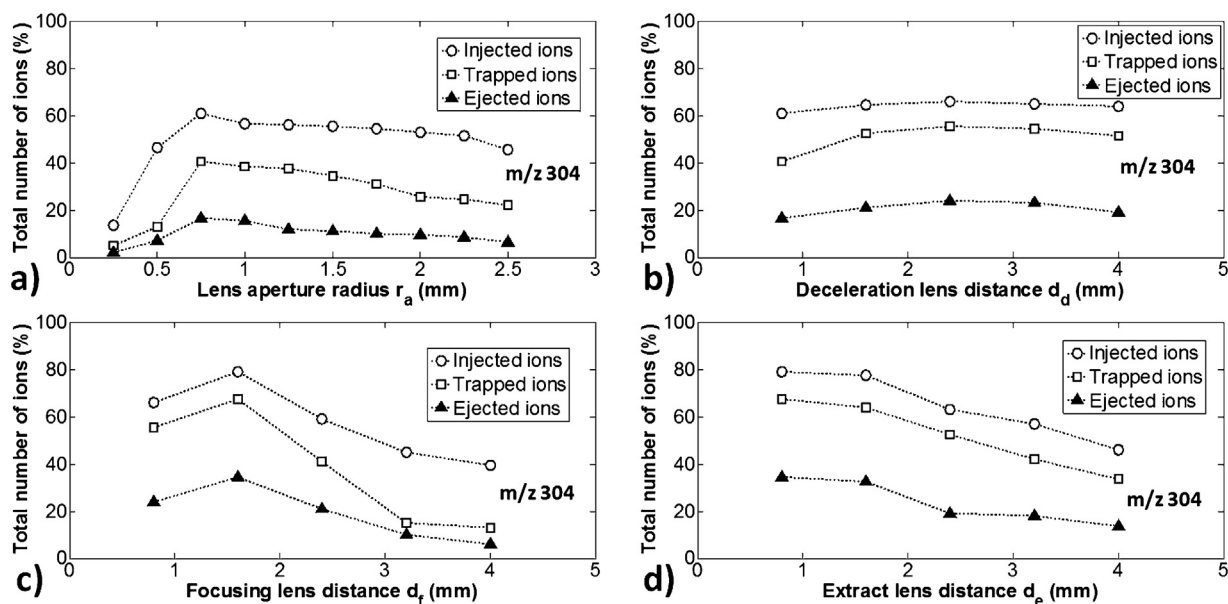
Fig. 7. Effects of varying ISLS geometrical parameters (r_a, d_d, d_f and d_e) on ion injection, trapping and ejection for cocaine at m/z 304 (3D simulations obtained using CPO).

4.2. Simulation results for cocaine ions

Fig. 6a shows the effect of lens aperture variation on ion injection, trapping and ejection from the total number of defined cocaine m/z 182 ions. As can be seen, the optimum lens r_a value is 0.75 mm ($0.3r_0$). To further improve ion focusing and maximize LIT sensitivity, distances between extract, focusing and deceleration lenses were also varied using optimal lens aperture radius. Effect of distance variation between the deceleration lens and entrance z-electrode is shown in Fig. 6b, where the optimum d_d value was found to be 2.4 mm ($6d$). Fig. 6c shows the effect of distance variation between the focusing and deceleration lenses with optimum d_f value of 1.6 mm ($4d$). Finally, the effect of distance variation between the extract and focusing lenses is shown in Fig. 6d with optimum d_e value of 0.8 mm ($2d$). It can be seen in Fig. 6a–d that ion injection, and particularly trapping efficiency and ion ejection have been greatly affected by altering the distances between the lenses. This is because the change of distances between the lenses has high impact on ion focusing, particularly between the focusing lens and entrance z-electrode.

Fig. 7a–d shows the results for cocaine m/z 304 ions with similar effects generated as for m/z 182. As can be seen, the optimal values for r_a, d_d, d_f and d_e are still the same as for m/z 182 with very similar output trends. Compared to standard lens system in a commercial ion source (SS Scientific Ltd.), simulation optimized ISLS shows sensitivity improvement by a factor of 4. Note that trapping efficiency in a non-scanning LIT is reduced when DC voltage is applied to the rods to narrow the mass window width, which reduces sensitivity. Also a number of ions are lost during ion ejection when a negative DC voltage is applied to exit z-electrode, which further reduces sensitivity. Therefore, the loss of ions during mass isolation and ion ejection from the LIT can be compensated for by improved ion injection through the optimized ISLS.

Space charge effects between ions were included in our simulations within the ISLS only, while no space charge was used within LIT. This is because CPO supports space charge for DC systems only, while no space charge effect is included for RF-driven systems like LITs. Fig. 8a and b shows trajectories for cocaine m/z 182 ions for commercial and simulation-optimized lens systems respectively using identical drive parameters. As
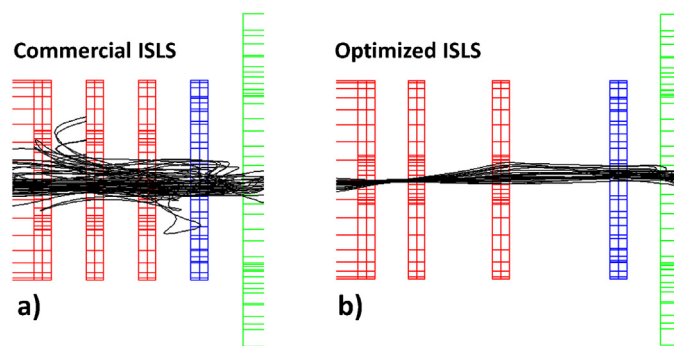

Fig. 8. Simulated ion trajectories in CPO for cocaine at m/z 182 for (a) commercial and (b) optimized ISLS.

can be seen, an optimized lens system with smaller aperture size and suitable lens spacing provides significantly better ion injection and focusing, which results in higher sensitivity of the analyzer.

5. Conclusions

Simulation results have shown considerable improvement in analyzer sensitivity by altering geometrical parameters of the ion source lens system coupled to a non-scanning linear ion trap. It was found that smaller lens aperture size was generally better for sensitivity, but not too small as ion transmission would be significantly reduced. Separation of the ion deceleration lens from the trap showed a moderate change in sensitivity. Distance alteration of the ion focusing lens had high impact on sensitivity with moderate lens separation shown to be the optimal one. Extract lens separation showed considerable change in sensitivity with minimal separation proven to be the best. With optimized lens distances, lower focusing voltages will be required, which will lead to lower ion injection energies and higher sensitivity. An optimized lens system also shows improvement in sensitivity by a factor of 4 compared to standard lens systems that have larger aperture sizes and minimal lens separations.

Acknowledgements

References

[1] A. Keil, H. Hernandez-Soto, R.J. Noll, M. Fico, L. Gao, Z. Ouyang, R.G. Cooks, Analytical Chemistry 80 (2008) 734.
[2] B. Brkić, N. France, S. Taylor, Analytical Chemistry 83 (2011) 6230.
[3] A. Keil, N. Talaty, C. Janfelt, R.J. Noll, L. Gao, Z. Ouyang, R.G. Cooks, Analytical Chemistry 79 (2007) 7734.
[4] N. Talaty, C.C. Mulligan, D.R. Justes, A.U. Jackson, R.J. Noll, R.G. Cooks, Analyst 133 (2008) 1532.
[5] S. Taylor, R.F. Tindall, R.R.A. Syms, Journal of Vacuum Science and Technology B 19 (2001) 557.
[6] B. Brkić, N. France, A.T. Clare, C.J. Sutcliffe, P.R. Chalker, S. Taylor, Journal of the American Society for Mass Spectrometry 20 (2009) 1359.
[7] K. Cheung, L.F. Velásquez-García, A.I. Akinwande, IEEE Journal of Microelectromechanical Systems 19 (2010) 469.
[8] D. Cruz, J.P. Chang, M. Fico, A.J. Guymon, D.E. Austin, M.G. Blain, Review of Scientific Instruments 78 (2007) 015107.
[9] A.T. Clare, L. Gao, B. Brkić, P.R. Chalker, S. Taylor, Journal of the American Society for Mass Spectrometry 21 (2010) 317.
[10] J.D. Maas, P.I. Hendricks, Z. Ouyang, R.G. Cooks, W.J. Chappell, IEEE Journal of Microelectromechanical Systems 19 (2010) 951.
[11] H.J. Yoon, J.H. Kim, E.S. Choi, S.S. Yang, K.W. Jung, Sensors and Actuators A 97–98 (2002) 441.
[12] E. Wapelhorst, J.P. Hauschild, J. Müller, Sensors and Actuators A 138 (2007) 22.
[13] S. Shimma, H. Nagao, J. Aoki, K. Takahashi, S. Miki, M. Toyoda, Analytical Chemistry 82 (2010) 8456.
[14] D.J. Douglas, A.J. Frank, D. Mao, Mass Spectrometry Reviews 24 (2005) 1.
[15] Y. Hashimoto, H. Hasegawa, T. Baba, I. Waki, Journal of the American Society for Mass Spectrometry 685 (17) (2006) 4.
[16] J.W. Hager, Journal of the American Society for Mass Spectrometry 20 (2009) 443.
[17] M. Guna, T.A. Biesenthal, Journal of the American Society for Mass Spectrometry 20 (2009) 1132.
[18] J.C. Schwartz, M.W. Senko, J.E.P. Syka, Journal of the American Society for Mass Spectrometry 13 (2002) 659.
[19] F.A. Londry, J.W. Hager, Journal of the American Society for Mass Spectrometry 14 (2003) 1130.
[20] C. Zhang, H. Chen, A.J. Guymon, G. Wu, R.G. Cooks, Z. Ouyang, International Journal of Mass Spectrometry 255–256 (2006) 1.
[21] P.H. Dawson, Mass Spectrometry Reviews 5 (1986) 1.
[22] F.H. Read, N.J. Bowring, Nuclear Instruments and Methods in Physics Research Section A 645 (2011) 273.
[23] B. Brkić, S. Taylor, J.F. Ralph, N. France, Physical Review A 73 (2006) 012326.
[24] A. Renau, F.H. Read, J.N.H. Brunt, Journal of Physics E: Scientific Instruments 15 (1982) 347.